

Potassic dyke swarm in the Sapucai Graben, eastern Paraguay: petrographical, mineralogical and geochemical outlines

P. Comin-Chiaromonti^a, A. Cundari^b, C.B. Gomes^c, E.M. Piccirillo^d, P. Censi^a, A. DeMin^d, G. Bellieni^e, V.F. Velazquez^c, D. Orué^f

^aIstituto di Mineralogia, Petrografia e Geochimica, Università di Palermo, Italy

^bSchool of Earth Sciences, University of Melbourne, Australia

^cInstituto de Geociencias, Universidade de São Paulo, Brazil

^dIstituto di Mineralogia e Petrografia, Università di Trieste, Italy

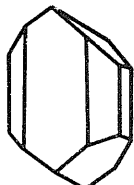
^eDipartimento di Mineralogia e Petrologia, Università di Padova, Italy

^fFacultad de Ciencias Exactas y Naturales, Universidad de Asunción, Paraguay

(Received May 20, 1991; revised and accepted March 5, 1992)

LITHOS

ABSTRACT



Comin-Chiaromonti, P., Cundari, A., Gomes, C.B., Piccirillo, E.M., Censi, P., DeMin, A., Bellieni, G., Velazquez, V.F. and Orué, D., 1992. Potassic dyke swarm in the Sapucai Graben, eastern Paraguay: petrographical, mineralogical and geochemical outlines. In: A. Peccerillo and S. Foley (Editors), Potassic and Ultrapotassic Magmas and their Origin. Lithos, 28: 283-301.

The western side of the Paraná Basin of Brazil extends to central Paraguay, where repeated and widespread magmatic activity developed from Lower Cretaceous to Oligocene, associated with late Mesozoic crustal extension trending NE-SW. In central Paraguay this trend is characterized by a zone of NW-SE normal faults which formed the Asunción-Sapucai graben, up to 45 km wide and 200 km long, where alkaline rocks occur as volcanic domes, complexes, lava-flows and dykes. These rocks, 128 Ma aged, are dominantly potassic and ne-normative.

A swarm of at least 200, mainly NW-SE trending, dykes occurs in the Sapucai region and seems to be formed by two main lineages: tephrite to phonolite (and peralkaline phonolite) and alkali basalt to trachyphonolite. They are characterized by ubiquitous diopside to ferrosilite, consistently yielding Al enrichment trends; common olivine, Fo_{81-69} in tephrites and alkaline basalts, and up to Fo_{65} in phonolites; zoned megacrysts of hastingsitic hornblende (core) to kaersutite (rim), associated with accessory groundmass pargasite in tephrites and phonotephrites; K-rich hastingsite and K-rich ferroan pargasite in the phonolites. Accessory groundmass mica falls in the annite-phlogopite range, and consistently yields insufficient ($Si + Al$) to satisfy the expected T site occupancy of 8.00 a.f.u. Fe-Ti oxides are Ti-magnetite, rarely ilmenite or haematite. Phenocrystal, i.e. xenocrystal plagioclase is An_{70-20} , and An_{74-42} in the tephrites and phonolites, respectively; coexisting groundmass microlites are An_{22-14} , associated with sodasanidine and sanidine. Feldspathoids include analcimized leucite and nepheline; accessories Ti-andradite and sphene.

The two main lineages, recognized by distinctive mineralogical variations, are consistent with the petrochemical variations. Complex interaction of discrete and independently evolving magma batches are indicated by intra- and/or interphase chemical variations, suggesting multiple equilibrations of the crystallizing phases under shallow level, volcanic pressure regime. The observed geochemical trends are quite similar to those of "Roman Region type magma" with the same negative anomalies of Ta, Nb, Zr and Ti. The most likely mantle source is a garnet-peridotite characterized by different enrichment in incompatible elements and which suffered low degree of partial melting (3-7%), which has geochemical and isotopic features distinct from those of the adjoining tholeiitic basalts (130 Ma) and nephelinites (61-39 Ma).

The similarities of the Sapucai dyke suite with Barton's "Roman Region type magma" supports the

Correspondence to: P. Comin-Chiaromonti, Istituto di Mineralogia, Petrografia e Geochimica, Università di Palermo, Italy.

view that this magma type may not be formed as a result of orogenic and/or subduction-driven activity in this region. Therefore, a causal relationship of the latter activity with "Roman Region type magma" is not supported and remains questionable.

Introduction and geological setting

The eruption of "continental flood basalts" and coeval alkaline magmas in western Gondwana is related with the opening of the Atlantic Ocean and is, therefore, fundamental in understanding the interaction between magma genesis and the dynamics of the lithosphere (Piccirillo and Melfi, 1988).

Alkaline rocks associated with rift-graben systems in the hinterland of the Paranà Basin of Brazil are relatively minor, compared with the "flood basalt" event. However, they are important in that they significantly extend the petrological spectrum of "basaltic suites" related to the splitting of the western Gondwana.

The western side of the central Paranà Basin, corresponding to eastern Paraguay, was the site of repeated and widespread magmatic activity from Lower Cretaceous to Oligocene times (Comin-

Chiaramonti et al., 1990b and references therein). "Landsat", aeromagnetic and gravity data indicate that the eastern Paraguay region was subjected to NE-SW trending crustal extension during the late Mesozoic (Degriff et al., 1981; Degriff, 1985; Mariano and Druecker, 1985; Druecker and Gay, 1987; Livieres and Quade, 1987).

The resulting faulting formed a complex NW-trending graben structure (25–45 km wide and 200 km long) in the Asunción-Sapucai region where alkaline rocks forming dykes, lava domes, lava flows and shallow-level intrusive complexes are unconformable on the Silurian sandstone of the "Caacupé Formation".

The alkaline rocks of the Asunción-Sapucai region represent the major occurrence of K-alkaline magmatism in Paraguay (Palmieri, 1973; Gomes et al., 1989) with K_2O/Na_2O mainly from 0.6 to 4.0. This region abuts Mesozoic tholeiitic volcanics of

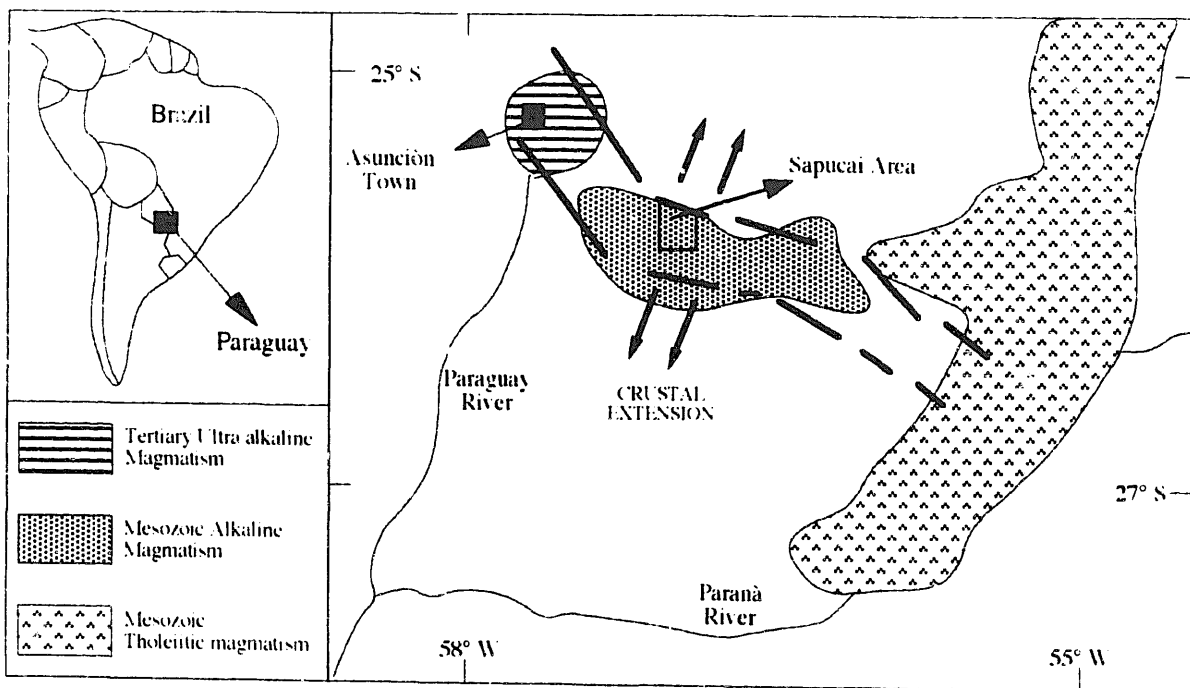


Fig. 1. Map of Asunción-Sapucai rift, Central-Eastern Paraguay, showing major areas of outcrops of igneous rocks, simplified from Bitschene (1987).

the "Serra Geral Formation" (130 Ma; Bitschene, 1987) on the eastern side and Tertiary (61–39 Ma) ultra-alkaline (sodic) rocks on the western side (Comin-Chiaromonti et al., 1991 and references therein). The potassic rocks (128 Ma; Velazquez et al., 1992) are close in time to continental splitting and rifting events which separated South America from Africa.

A mainly NW–SE trending dyke swarm of at least 200 dykes, 0.5 to 20 m thick, formed by alkaline assemblages, is concentrated near Sapucaí town (Fig. 1). A systematic study of these rocks was initiated with the view of identifying petrological features characteristic of magmas undoubtedly related to a regime of continental rifting, where subcontinental mantle sources generated differentiated potassic suites of "low volcanicity", consistent with that of the "Serra Geral flood basalts". The origin and evolution of these sources may reflect specific geochemical characteristics of the lithospheric/asthenospheric mantle.

This paper presents essential mineralogical and bulk data necessary to delineate the features of the Sapucaí dyke swarm. Detailed petrography and a mineral chemistry data are in Gomes et al. (1989) and in Comin-Chiaromonti et al. (1990a,b), or are available on request.

Analytical procedures

Mineral analyses were made on a ARL-SEMQ instrument at Cagliari University, operating at 15 kV and 20 nA. The standards were of oxides or simple silicate compositions. Major and trace element analyses of whole-rocks have been carried out at the Trieste University by X-ray fluorescence techniques using a Philips PW/1400 spectrometer on pressed-powder pellets. The preparation methods and analytical procedures have been described by Bellieni et al. (1983).

REE, Th and U of some selected samples were measured on a Perkin-Elmer ScieX Elan 500 mass spectrometer (upgrade to 5000), at CEPA s.r.l. (Palermo), following the procedures described by Alaimo and Censi (1992). Seven-point (1 to 500 ppb) multi-element calibration standard solutions were used to calculate elemental concentrations. Rh (210.6 ppb) was used as internal standard to compensate for any changes in analyzed signals.

Petrography and mineral chemistry

Following the classification of De La Roche et al. (1980), the mesozoic dyke swarm of the Sapucaí area can be divided into two main lineages (Fig. 2):

(1) a silica-undersaturated lineage ranging from tephrites to phonolites and peralkaline phonolites;

(2) a silica-saturated lineage ranging from alkali basalts to trachyphonolites.

The majority of the rock-types are notably porphyritic with between 10 and 40% phenocrysts + microphenocrysts set in hypohyaline to hypocrystalline groundmass.

(1) The first lineage

The generalized mineral assemblage in *tephrites* and *phonotephrites* is clinopyroxene + olivine + feldspars + feldspathoids (major constituents), Fe-Ti oxides + mica ± amphibole (minor constituents) and accessory apatite, zircon and rare carbonates. Included in this group are rare rock-types with seriate mica + clinopyroxene (up 2 cm across) set in a glassy groundmass with microlites of clinopyroxene + mica + Fe-Ti oxides + feldspathoids (*minette*, according to Bergman, 1987 and Le Maitre, 1989).

Assuming $\text{FeO}/\text{Fe}_2\text{O}_3 = 0.17$, then:

Minette: $\text{MgO}/(\text{MgO}+\text{FeO}) = \text{Mg\#} = 0.73\text{--}0.70$; CIPW Ne = 13–15%; $(\text{Na}+\text{K})/\text{Al} = 0.75$; $\text{K}_2\text{O}/\text{Na}_2\text{O} = 1.3\text{--}1.5$.

Tephrite: $\text{Mg\#} = 0.68\text{--}0.48$; CIPW Ne = 10–20%; $(\text{Na}+\text{K})/\text{Al} = 0.65\text{--}0.75$; $\text{K}_2\text{O}/\text{Na}_2\text{O} = 0.9\text{--}1.9$.

Phonotephrite: $\text{Mg\#} = 0.60\text{--}0.47$; CIPW Ne = 10–18% and CIPW Lc 0–14%; $(\text{Na}+\text{K})/\text{Al} = 0.62\text{--}0.88$; $\text{K}_2\text{O}/\text{Na}_2\text{O} = 1.2\text{--}1.9$.

Phonolites have clinopyroxene + alkali feldspar + feldspathoids ± plagioclase ± olivine ± andradite ± sphene set in a glassy matrix. Mica and Fe-Ti oxides are uncommon, amphibole is rare. They are distinguished in:

A-type: pseudoleucite megacrysts; $\text{MgO} > 3$ wt. %; CIPW Ne = 17–27% and CIPW Lc = 0–24%; $(\text{Na}+\text{K})/\text{Al} = 0.95\text{--}0.96$; $\text{K}_2\text{O}/\text{Na}_2\text{O} = 1.2\text{--}2.3$ (up to group III ultrapotassic rock-types of Foley et al., 1987);

B-type: plagioclase megacrysts; $\text{MgO} = 1.5\text{--}3.0$ wt. %; CIPW Ne = 12–13%; $(\text{Na}+\text{K})/\text{Al} = 0.70\text{--}0.74$; $\text{K}_2\text{O}/\text{Na}_2\text{O} = 1.4\text{--}2.0$;

C-type: alkali feldspar and nepheline megacrysts; $\text{MgO} < 1.5$ wt. %; CIPW Ne = 22–28%; $(\text{Na}+\text{K})/\text{Al} = 0.90\text{--}0.94$; $\text{K}_2\text{O}/\text{Na}_2\text{O} = 0.75\text{--}0.77$;

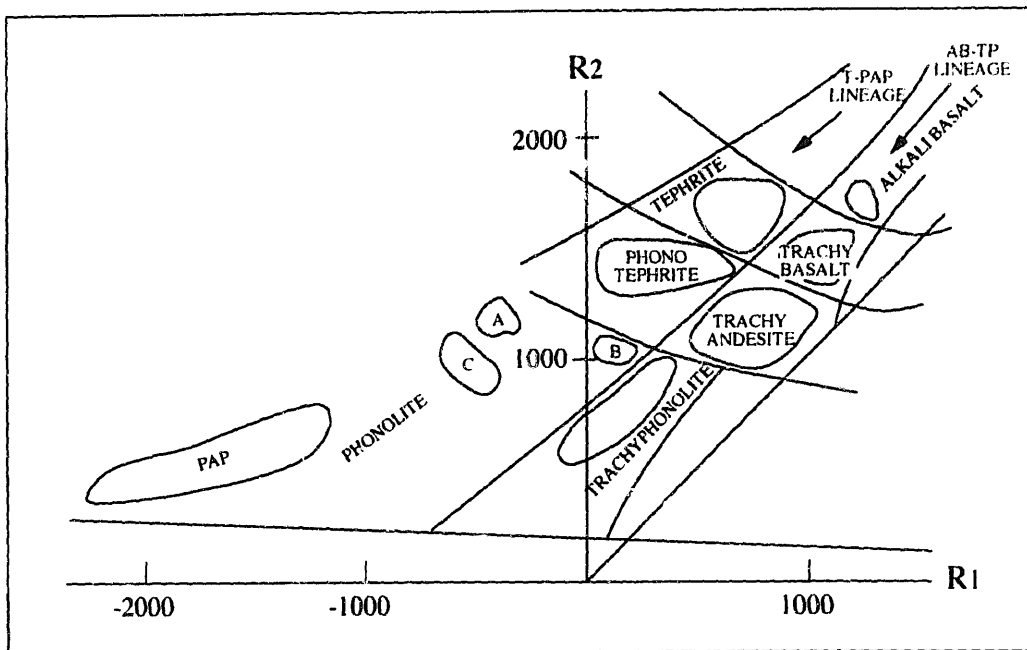


Fig. 2. R_1 - R_2 plot ($R_1 = 4\text{Si} - 11(\text{Na} + \text{K}) - 2(\text{Fe} + \text{Ti})$, $R_2 = 6\text{Ca} + 2\text{Mg} + \text{Al}$; De La Roche et al., 1980) with the main fields of potassic rock-types from the Sapucaí dyke swarm. *T-PAP*, tephrite to phonolite (A-, B-, C-type and peralkaline phonolites) and *AB-TP*, alkali basalt to trachyphonolite lineages, respectively.

Peralkaline: garnet and sphene microphenocrysts; $\text{MgO} < 0.5$ wt. %; CIPW Ne=29–33%; $(\text{Na} + \text{K})/\text{Al} = 1.1\text{--}1.3$; $\text{K}_2\text{O}/\text{Na}_2\text{O} = 0.62\text{--}0.71$.

(2) The second lineage

In the *alkaline basalt to trachyphonolite* lineage, clinopyroxene is the most abundant constituent, associated with plagioclase + alkali feldspar; olivine occurs in alkali basalts and in trachybasalts; mica is a common groundmass microlite, rarely phenocryst–microphenocryst in trachybasalts and trachyphonolites. Amphibole phenocrysts occur in the latter. Fe-Ti oxides are ubiquitous microphenocrysts and microlites. Phenocryst–microphenocryst sphene occurs in trachyphonolites; apatite and zircon are common accessories in all rock-types.

Alkaline basalt: Mg#=0.63–0.56; CIPW Ne=4–7%; $(\text{Na} + \text{K})/\text{Al} = 0.51\text{--}0.56$; $\text{K}_2\text{O}/\text{Na}_2\text{O} = 0.64\text{--}1.54$;

Trachybasalt: Mg#=0.65–0.51; CIPW Ne=3–8%; $(\text{Na} + \text{K})/\text{Al} = 0.46\text{--}0.70$; $\text{K}_2\text{O}/\text{Na}_2\text{O} = 0.65\text{--}2.50$ (up to group III ultrapotassic rock-types, according to Foley et al., 1987).

Trachyphonolites: Mg#=0.37–0.22; CIPW Ne=8–10%; $(\text{Na} + \text{K})/\text{Al} = 0.71\text{--}0.87$; $\text{K}_2\text{O}/\text{Na}_2\text{O} = 1.00\text{--}1.90$.

Mineral chemistry

Clinopyroxene. Representative clinopyroxene analyses are given in Table 1. The highest Ca occurs in clinopyroxene from the more silica undersaturated rock compositions, the late-crystallized microphenocryst and groundmass clinopyroxene forming a characteristic Ca- and Fe-enrichment trend (Fig. 3). The Ti/Al ratio of the clinopyroxene from the minette and tephrites ($\text{Ti}/\text{Al} = 0.19\text{--}0.33$) virtually overlaps the corresponding range for the clinopyroxene from phonotephrites ($\text{Ti}/\text{Al} = 0.14\text{--}0.35$), the highest Ti/Al values matching the highest $(\text{Na} + \text{K})/\text{Al}$ ratio of the bulk rocks (i.e. > 0.70). Clinopyroxene from single specimens often display the whole Ti/Al variation reported for the tephrite–phonotephrite clan.

Megacryst compositions in A-phonolites are virtually identical to the above, whereas B- and C-phonolites contain augite ($\text{Ti}/\text{Al} = 0.16\text{--}0.20$) and salite ($\text{Ti}/\text{Al} = 0.17\text{--}0.30$) megacrysts, respectively. Peralkaline phonolites are characterized by megacrysts similar to the latter in composition, but mantled by ferrosilite rims ($\text{Ti}/\text{Al} = 0.11\text{--}0.18$), matching the coexisting phenocrystal and ground-

Table 1 - Representative compositions of clinopyroxenes. M, P, mP and GM : megacrystals (>10 mm), phenocrystals (1-5 mm), microphenocrysts (0.2-1mm) and microlites, respectively. Structural formulae on the basis of 4 Cations and 6 Oxygens.

	MINETTE			TEPHRITE			PHONOTEPHRITE			A-PHONOLITE		B-PHONOLITE		C-PHONOLITE	
	M	GM	M	mP	GM	M	P	mP	GM	M	GM	M	P	M	GM
SiO ₂	53.55	49.31	49.69	50.68	46.14	53.93	49.17	48.22	43.75	50.33	45.80	49.76	51.41	46.58	46.57
TiO ₂	0.67	1.94	1.34	1.68	2.48	0.26	1.72	2.16	4.70	1.23	3.40	1.18	0.98	1.55	1.41
Al ₂ O ₃	1.28	4.11	3.94	3.74	7.36	1.16	5.18	4.54	9.92	3.03	6.66	3.89	5.10	5.91	4.99
FeO	4.96	7.52	8.04	5.96	9.57	4.05	7.36	7.30	10.91	6.01	8.95	8.21	9.19	11.67	11.58
MnO	0.12	0.09	0.17	0.18	0.22	0.00	0.44	0.18	0.24	0.14	0.24	0.42	0.10	0.47	0.32
MgO	17.00	14.57	14.57	14.57	11.94	17.79	13.45	12.99	9.73	14.74	11.45	14.60	13.70	9.65	10.08
CaO	22.26	22.31	21.86	22.78	21.46	22.29	22.21	23.05	20.08	22.91	22.14	21.08	21.31	22.22	22.22
Na ₂ O	0.55	0.00	0.39	0.38	0.76	0.18	0.47	0.59	0.60	0.34	0.63	0.78	0.22	0.94	0.87
Cr ₂ O ₃	0.05	0.14	0.00	0.04	0.05	0.36	0.00	0.02	0.07	0.08	0.00	0.09	0.00	0.00	0.01
Σ	100.44	99.99	100.00	99.63	99.98	100.02	100.00	99.05	100.00	98.81	99.27	100.01	100.01	98.99	98.35
Fe ₂ O ₃ *	2.11	1.62	3.75	1.04	5.13	0.47	2.30	3.33	0.51	2.29	3.40	5.24	0.60	5.64	6.39
Si	1.945	1.831	1.839	1.870	1.724	1.963	1.823	1.808	1.658	1.878	1.730	1.836	1.917	1.776	1.786
Al IV	0.055	0.169	0.161	0.130	0.276	0.037	0.177	0.192	0.342	0.122	0.270	0.164	0.083	0.224	0.216
Σ	2.000	2.000	2.000	2.000	2.000	2.000	2.000	2.000	2.000	2.000	2.000	2.000	2.000	2.000	2.000
Al VI	0.000	0.011	0.013	0.033	0.047	0.012	0.049	0.009	0.101	0.011	0.026	0.006	0.054	0.042	0.012
Fe++	0.093	0.188	0.144	0.155	0.155	0.110	0.164	0.126	0.331	0.123	0.186	0.108	0.287	0.210	0.187
Fe+++	0.058	0.045	0.104	0.029	0.144	0.013	0.065	0.103	0.015	0.064	0.097	0.146	0.000	0.162	0.184
Mg	0.920	0.806	0.803	0.801	0.664	0.965	0.743	0.726	0.550	0.820	0.644	0.803	0.761	0.549	0.576
Mn	0.004	0.003	0.005	0.006	0.007	0.000	0.013	0.006	0.008	0.004	0.008	0.013	0.003	0.015	0.017
Ti	0.018	0.054	0.037	0.047	0.070	0.007	0.048	0.061	0.134	0.035	0.097	0.033	0.028	0.044	0.041
Cr	0.001	0.004	0.000	0.001	0.001	0.010	0.000	0.001	0.002	0.002	0.000	0.003	0.000	0.000	0.000
Ca	0.866	0.888	0.867	0.901	0.858	0.869	0.882	0.926	0.815	0.916	0.896	0.834	0.852	0.908	0.918
Na	0.041	0.000	0.028	0.027	0.055	0.013	0.034	0.043	0.044	0.025	0.046	0.056	0.016	0.070	0.065
Σ	2.001	1.999	2.001	2.000	2.001	2.000	2.000	2.001	2.000	2.000	2.000	2.000	2.001	2.000	2.000
Ca	44.6	46.0	45.1	47.6	46.9	44.4	47.2	49.1	47.4	47.5	48.9	43.8	44.8	49.2	48.8
Mg	47.4	41.6	41.7	42.3	36.3	49.3	39.8	38.5	32.0	42.6	35.2	42.2	40.0	29.8	30.6
Fe**	8.0	12.2	13.2	10.1	16.8	6.3	13.0	12.4	20.6	9.9	15.9	14.0	15.2	21.0	20.6
mg#	0.908	0.811	0.848	0.838	0.811	0.898	0.819	0.852	0.624	0.869	0.776	0.881	0.726	0.723	0.755
PERALKALINE PHONOLITE			ALKALINE BASALT			TRACHYBASALT					TRACHYPHONOLITE				
M	P	GM	M	GM	M1	M2	P	P	GM	GM	P	GM	GM		
SiO ₂	48.02	48.67	50.85	52.45	49.43	53.58	51.54	50.77	50.32	50.57	50.83	49.90	47.60	52.00	
TiO ₂	1.71	0.73	2.22	0.29	1.22	0.13	0.50	0.74	0.93	0.97	1.25	1.42	1.89	0.45	
Al ₂ O ₃	4.67	2.94	1.57	2.03	4.20	0.01	2.98	2.92	4.52	5.60	3.12	3.29	5.03	1.36	
FeO	9.33	17.52	24.75	4.29	9.94	8.57	4.62	6.36	8.03	9.08	7.78	9.24	11.28	15.13	
MnO	0.39	1.61	1.75	0.05	0.19	0.27	0.12	0.16	0.22	0.32	0.40	0.34	0.37	0.68	
MgO	12.67	6.66	1.00	16.75	13.30	14.11	15.78	14.83	14.37	11.55	13.43	11.84	10.12	8.55	
CaO	22.55	20.22	9.24	23.33	21.50	22.70	22.38	22.53	21.42	21.00	22.14	23.23	22.69	19.62	
Na ₂ O	0.35	1.58	8.47	0.00	0.12	0.38	0.38	0.32	0.12	1.87	0.99	0.68	0.88	2.75	
Cr ₂ O ₃	0.31	0.02	0.00	0.80	0.11	0.01	0.86	0.21	0.08	0.02	0.05	0.04	0.02	0.00	
Σ	100.00	99.95	99.85	99.99	100.01	99.76	99.16	98.84	100.01	100.98	99.99	99.98	99.88	100.54	
Fe ₂ O ₃ *	4.29	6.13	18.45	1.23	1.93	1.10	0.88	2.14	0.95	4.69	3.52	2.96	4.69	7.07	
Si	1.797	1.882	1.949	1.920	1.849	1.998	1.904	1.894	1.865	1.854	1.883	1.869	1.799	1.957	
Al IV	0.203	0.118	0.051	0.080	0.151	0.001	0.096	0.106	0.135	0.146	0.117	0.131	0.201	0.043	
Σ	2.000	2.000	2.000	2.000	2.000	1.999	2.000	2.000	2.000	2.000	2.000	2.000	2.000	2.000	
Al VI	0.003	0.017	0.020	0.007	0.034	0.000	0.034	0.022	0.063	0.096	0.019	0.014	0.023	0.017	
Fe++	0.171	0.388	0.261	0.098	0.257	0.237	0.106	0.133	0.223	0.149	0.143	0.206	0.223	0.276	
Fe+++	0.121	0.178	0.532	0.034	0.054	0.091	0.037	0.060	0.027	0.129	0.098	0.083	0.133	0.200	
Mg	0.706	0.384	0.057	0.914	0.741	0.784	0.858	0.324	0.794	0.631	0.741	0.66	0.570	0.480	
Mn	0.012	0.053	0.057	0.002	0.006	0.009	0.004	0.005	0.007	0.010	0.013	0.011	0.012	0.022	
Ti	0.048	0.021	0.064	0.008	0.034	0.004	0.014	0.021	0.026	0.027	0.035	0.040	0.054	0.013	
Cr	0.009	0.001	0.000	0.023	0.003	0.000	0.025	0.006	0.002	0.001	0.001	0.002	0.001	0.000	
Ca	0.904	0.838	0.380	0.915	0.862	0.907	0.885	0.900	0.850	0.825	0.879	0.933	0.919	0.791	
Na	0.025	0.120	0.628	0.000	0.009	0.027	0.027	0.023	0.008	0.133	0.071	0.049	0.065	0.201	
Σ	2.000	2.000	2.000	2.000	2.000	1.999	2.000	1.999	2.000	2.001	2.000	1.999	2.000	2.000	
Ca	47.2	45.5	29.5	46.6	44.9	46.1	46.6	46.7	44.7	47.3	46.9	49.3	49.5	44.7	
Mg	36.9	20.9	4.4	46.6	38.6	39.8	45.7	42.8	41.8	36.2	39.5	34.9	30.7	27.1	
Fe**	15.9	33.6	66.1	6.8	16.5	14.1	7.7	10.5	13.5	16.5	13.6	15.8	19.8	28.2	
mg#	0.805	0.497	0.179	0.903	0.742	0.768	0.891	0.857	0.781	0.809	0.838	0.762	0.719	0.635	

Fe₂O₃* calculated from stoichiometry; Fe⁺⁺=Fe²⁺+Fe³⁺+Mn; mg#=Mg/(Mg+Fe²⁺).

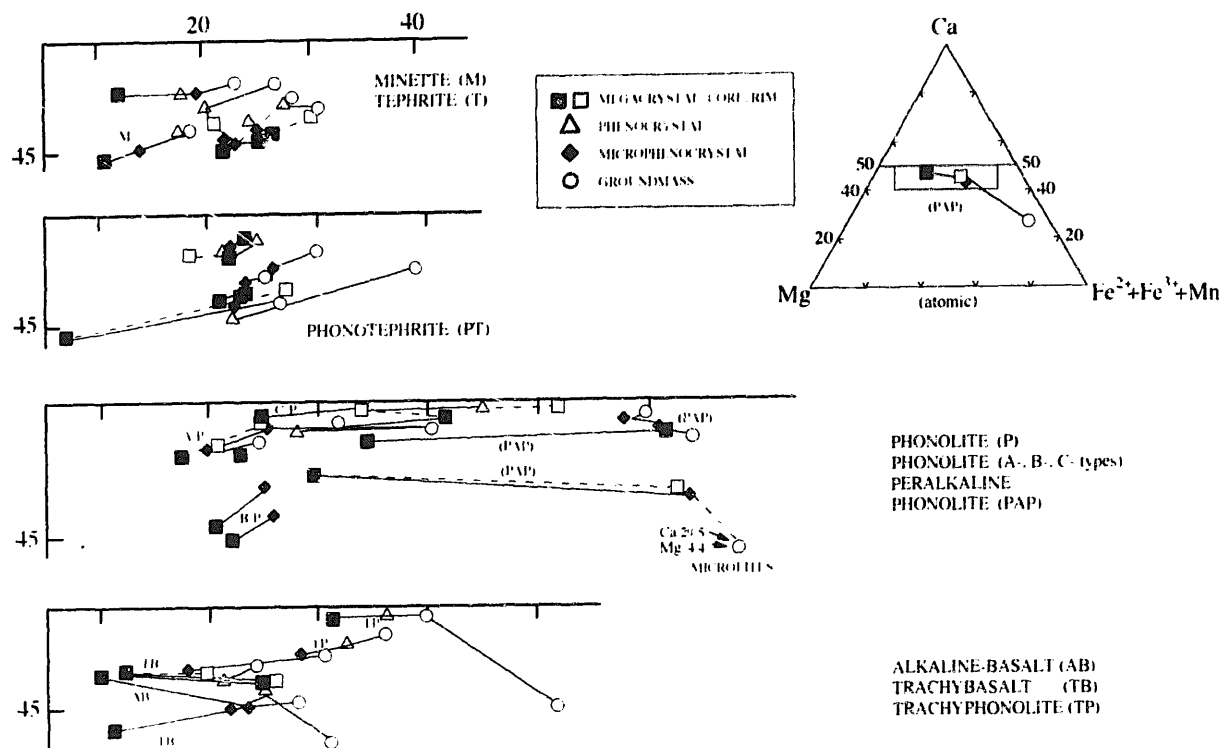


Fig. 3. Compositions of clinopyroxene in the various clans. Tie lines connect coexisting clinopyroxenes.

mass pyroxene. Microlites in these rocks are aegirine-augite (acmite up to 63% mol; Ti/Al up to 0.90).

The clinopyroxene from the alkali basalt-trachyphonolite lineage is generally similar to that in the tephrite-phonotephrite clan. As in the latter, megacrysts show diopsidic cores mantled by salite rims. Two distinct megacryst generations were observed, i.e. diopside and salite with $(Si + Al) < 2.00$ and $(Si + Al) > 2.00$, corresponding to $Ti/Al = 4$ and 0.11, respectively. The former megacrysts probably crystallized from liquid compositions with $(Na + K) > 1$ (Cundari and Ferguson, 1982).

Olivine. Olivine (Table 2) is commonly microphenocryst to groundmass phase (Fo_{76-68}) in tephrites and megacryst to microphenocryst (Fo_{79-70}) in phonotephrites. Microphenocrysts or groundmass olivine is present only in A- and B-phonolites (Fo_{75-65}). Olivine megacryst up to microphenocrysts occur also in alkali basalts and trachybasalts (Fo_{82-56}), attaining Fo_{48} in the microlites from the trachybasalt groundmass.

Olivine compositions appear to be in broad equilibrium with the coexisting clinopyroxene, but me-

gacrysts and phenocrysts from phonotephrites yielded higher forsterite than the expected equilibrium temperatures.

In general, close chemical correlations apply only to the olivine-clinopyroxene pairs from tephrite-phonotephrite and phonolite dykes, reflecting their cognate relationships, whereas there is poor linear correlation for $Fe_t/(Fe_t + Mg)$ values between coexisting olivine and clinopyroxene compositions in alkali basalt-trachybasalt rock-types.

Fe-Ti oxides. Magnetite-ulvöspinel solid solutions occur as microphenocrysts and groundmass constituents; coexisting magnetite-ilmenite pairs were rarely observed as microlites in tephrites, phonotephrites, B-phonolites, being more common in alkali basalts (Table 3) and generally indicate T °C and f_{O_2} conditions above the QMF buffer curve (Fig. 4). Haematite is a common groundmass constituent in peralkaline phonolites, but also mantling and/or replacing magnetite in the other rock-types. Notably, Ti-magnetite with decreasing ulvöspinel proportion, i.e. 73 to 9 mol%, was observed in alkali basalt to trachyphonolite rock-types.

Similar to the tephrite-phonotephrite and phon-

Table 2 - Representative compositions of olivine. Letters as in Table 1. Structural formulas on the basis of 4 Oxygens.

	TEPHRITE			PHONOTEPHRITE			PHONOLITE			ALKALINE BASALT			TRACHYBASALT		
	P	mP	GM	M	P	mP	A-type		B-type		P	GM	M	mP	GM
							mP	GM	mP	GM					
SiO ₂	38.42	38.41	37.39	39.39	38.92	37.60	38.21	38.06	36.92	39.24	37.81	39.51	38.08	34.63	
FeO	21.77	21.79	27.43	18.49	20.38	26.21	21.34	23.56	29.42	17.53	27.21	16.47	24.03	41.37	
MnO	0.34	0.50	0.58	0.49	0.56	0.39	0.58	0.71	0.74	0.38	0.62	0.31	1.26	1.02	
MgO	38.90	38.40	33.88	41.59	39.79	35.09	38.31	36.87	32.09	42.19	34.57	43.20	36.56	22.12	
CaO	0.29	0.28	0.58	0.40	0.66	0.36	0.63	0.54	0.53	0.26	0.52	0.46	0.21	0.63	
Σ	99.72	99.78	99.86	100.36	100.31	99.65	99.07	99.74	99.70	99.60	100.73	99.95	100.14	99.81	
Si	0.998	1.000	1.000	1.001	1.000	1.000	1.000	1.000	1.000	1.000	1.000	0.999	1.000	1.000	
Fe ⁺⁺	0.471	0.473	0.611	0.392	0.436	0.581	0.465	0.516	0.664	0.372	0.599	0.347	0.526	0.996	
Mn	0.007	0.020	0.013	0.011	0.012	0.009	0.013	0.016	0.017	0.008	0.014	0.007	0.028	0.025	
Mg	1.516	1.500	1.359	1.585	1.533	1.400	1.504	1.453	1.304	1.613	1.372	1.638	1.440	0.960	
Ca	0.008	0.008	0.017	0.011	0.018	0.010	0.018	0.015	0.015	0.007	0.015	0.012	0.006	0.019	
Σ	3.000	3.001	3.000	3.000	2.999	3.000	3.000	3.000	3.000	3.000	3.000	3.003	3.000	3.000	
Fo	75.72	74.96	67.95	79.29	76.69	70.00	75.20	72.65	65.20	80.65	68.60	81.73	72.00	48.00	
Fa	23.53	23.64	30.55	19.61	21.81	29.05	23.25	25.86	33.20	18.59	29.95	17.32	26.30	49.80	
Tph	0.35	1.00	0.65	0.55	0.60	0.45	0.65	0.80	0.85	0.40	0.70	0.35	1.40	1.25	
Lar	0.40	0.40	0.85	0.55	0.90	0.50	0.90	0.75	0.75	0.35	0.75	0.60	0.30	0.95	
mg#	0.763	0.760	0.690	0.802	0.779	0.707	0.764	0.738	0.663	0.813	0.696	0.825	0.732	0.401	

$$\text{mg\#} = \text{Mg}/(\text{Mg}+\text{Fe}^{2+})$$

elite assemblages, Ti-magnetite from the Vico and Sabatini leucite-tephrite/phonolite suite, Roman Region, contains $\text{TiO}_2=8\text{--}17\%$, in absence of co-existing ilmenite (Cundari, 1975; 1979).

Mica. Mica is a Ti-rich member of the annite-phlogopite series (Table 4; Fig. 5A). The $\text{Fe}_2\text{O}_3/\text{FeO}$ ratios, estimated from charge balance, are consistently higher in the mica from first lineage (2.1–15.0) than the $\text{Fe}_2\text{O}_3/\text{FeO}$ ratios in the mica from the second one (0.5–0.9); systematically $(\text{Si}+\text{Al}) < 8.00$ a.f.u., with Ti completing the occupancy of the T sites.

Likewise, mica from Vico and Sabatini leucite-tephrite/phonolite suites is phlogopite, generally with $(\text{Si}+\text{Al}) > 8.00$, but also $(\text{Si}+\text{Al}) < 8.00$ and $\text{TiO}_2=2\text{--}5$ wt. % (Cundari, 1975; 1979). Virtually identical compositions were reported by Holm (1982) for mica occurring in leucite-tephrite/leucites from the Vulsini complex, Roman Region. Mica from tephrite to phonolite lineage is higher in Ti ($\text{TiO}_2=5\text{--}8$ wt. %) compared with mica from the above Roman Region lavas, but is close to the range ($\text{TiO}_2=4\text{--}7$ wt. %) reported for mica in southwestern Ugandan phonolitic tephrite series (Ferguson, 1978).

Ti-rich mica, phenocryst, microphenocryst and microilites occurring in trachybasalts and trachy-phonolites has compositions fitting the magnetite-haematite buffer (Fig. 5B), whereas the mica from minette-tephrite-phonotephrite and phonolite-

peralkaline phonolite clans is clearly removed from the regions of buffered compositions, suggesting that mica crystallization in the corresponding liquids may have occurred under unbuffered conditions.

Amphibole. Pargasitic amphibole is an accessory groundmass phase in the tephrite-phonotephrite rock-types, and may coexist with megacryst amphibole varying from hastingsitic hornblende (core) to kaersutite (rim), according to Leake's nomenclature (Table 5). Similar to mica, all the analyzed amphiboles are characterized by $(\text{Si}+\text{Al}) < 8.00$ a.f.u. and Ti may complete the occupancy of the T sites. Notably, the sum of cations, based on 23 oxygens is less than the expected 16 a.f.u., Ca is restricted to M4 and the occupancy of the A site is low ($\text{Na}+\text{K}=0.8\text{--}0.9$ a.f.u.), K/Na varying in the range 0.4–0.5. These crystal chemical characteristics are shared with amphiboles in tephritic lavas from Sabatini (Cundari, 1979) and Vulsini lavas (Holm, 1982) and the Cordon Complex, Philippines (Knittel and Cundari, 1990).

A more extensive amphibole crystallization, relative to the tephrites-phonotephrites, is indicated for the C- and peralkaline phonolites, where the full textural range, from megacryst K-rich ferroan pargasite to groundmass, K-rich Mg-hastingsite, is represented (Table 5, Fig. 6). The T site is completed by $(\text{Si}+\text{Al})$; the sum of cations, based on 23 oxygens, exceeds 16 a.f.u., averaging 16.067 ± 0.087 ; $(\text{Na}+\text{K}) > 1$ a.f.u. and $\text{K}/\text{Na}=0.7\text{--}0.9$.

Ferroan pargasite phenocrysts, microphenocrysts

TABLE 3

Representative compositions of Fe-Ti oxides. Fe_2O_3 and FeO calculated on ulvöspinel and ilmenite basis for cubic and rombohedral phases and structural formula on the basis of 32 and 3 Oxygens, respectively

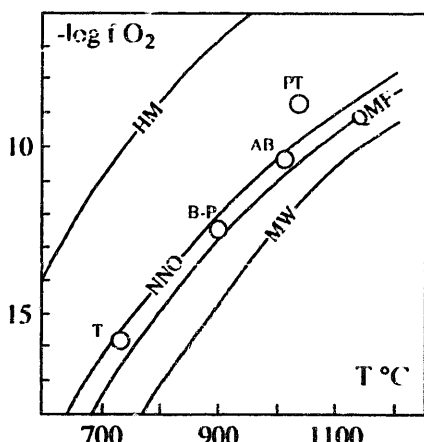


Fig. 4. Stability relations in f_{O_2} - T °C space for magnetite-ilmenite pairs. Abbreviations and symbols as in Fig. 3. Buffers are from Speer and Lindsley (1981)

and microlites also occur in trachyphonolites. Occupancy of the A site, K/Na ratio, Ti and calculated Fe^{3+} values are intermediate between the analogues for amphiboles in tephrites and phonolites.

Feldspars. Zoned plagioclase phenocrysts and microphenocrysts (An_{70-20}) prevail in hypocrystalline assemblages of the tephrite-phonotephrite clan,

coexisting with late-crystallized oligoclase (An_{20-14}). Sodic sanidine (Ab_{39}) and/or albite patches occur in tephrites; sanidine (Ab_{17-18}) and/or sodic sanidine (Ab_{40-43}) microlites in phonotephrites. Plagioclase megacrysts (An_{74-42}) to microphenocrysts (An_{64-26}), commonly mantled by sodic sanidine (c. Ab_{40}), were only observed in B-phonolites and are considered as xenocrysts. Rare microphenocrysts and groundmass plagioclase (An_{22-16}) were observed in A-phonolites, while none was detected in C-phonolites. Feldspars from phonolitic rocks follow Ca-depletion, Na-, K-enrichment trends, and Ca-, Na-depletion and K-enrichment trends, for plagioclase and alkali feldspar, respectively, consistent with the feldspar crystallization trends in leucite-bearing rocks from the Roman Region (Ferguson and Cundari, 1982).

Alkali basalt-trachybasalt assemblages are characterized by zoned microphenocrysts (An_{69-30}) and homogeneous plagioclase (An_{26-20}) and alkali feldspar (Or_{52}) microlites. Plagioclase megacrysts (An_{13-12}) occur in trachyphonolites, where the groundmass feldspar is typically sanidine/Na-sanidine.

Feldspathoids. Euhedral analcime and/or pseu-

Table 4 - Representative compositions of micas. Structural formulae on the basis of 22 Oxygens and Fe_2O_3 as from charge balance.

MINETTE		PHONO TEPHRITE		PHONOLITE			TRACHY BASALT		TRACHY PHONO		
		Mc	Mr	GM	GM	A-type	B-type	GM	P	mP	GM
SiO_2	38.78	36.82	35.42	36.61	35.10	36.24	36.00	38.35	38.00	36.97	
TiO_2	5.86	5.23	7.06	6.82	8.57	7.85	6.95	8.49	8.07	7.87	
Al_2O_3	15.04	15.05	13.62	14.30	15.55	13.70	14.85	14.33	14.19	14.81	
FeO	11.19	17.09	18.64	16.09	14.99	18.28	14.29	11.30	12.78	16.94	
MnO	0.12	0.26	0.29	0.32	0.23	0.30	0.26	0.11	0.34	0.21	
MgO	17.78	14.05	13.19	14.20	13.24	9.31	13.87	14.90	13.88	10.94	
CaO	0.00	0.00	0.03	0.01	0.02	0.04	0.04	0.05	0.00	0.03	
Na_2O	0.13	0.00	0.66	0.25	0.52	0.64	0.66	0.58	0.45	0.50	
K_2O	8.37	8.45	8.53	8.51	8.75	9.70	9.37	8.58	8.56	8.43	
Cr_2O_3	n.d.	n.d.	0.04	0.03	0.00	0.00	0.03	0.07	0.00	0.03	
Σ	97.27	96.95	97.48	97.14	96.97	96.06	96.32	96.65	96.27	95.73	
Fe_2O_3	9.90	12.34	16.15	11.78	11.11	10.37	14.80	5.70	5.63	6.08	
Si	5.396	5.274	5.084	5.237	5.036	5.362	5.149	5.451	5.467	5.459	
Al IV	2.467	2.541	2.304	2.411	2.630	2.389	2.503	2.401	2.407	2.404	
Ti	0.137	0.185	0.612	0.352	0.334	0.249	0.348	0.148	0.126	0.137	
Σ	8.000	8.000	8.000	8.000	8.000	8.000	8.000	8.000	8.000	8.000	
Al VI	0.000	0.000	0.000	0.000	0.000	0.000	0.000	0.000	0.000	0.000	
Fe^{++}	0.265	0.716	0.492	0.657	0.599	1.108	0.116	0.733	0.928	1.417	
Fe^{+++}	1.037	1.330	1.745	1.268	1.200	1.155	1.593	0.610	0.610	0.675	
Mg	3.688	3.000	2.822	3.028	2.831	2.054	2.957	3.136	2.977	2.406	
Mn	0.014	0.031	0.035	0.039	0.028	0.038	0.032	0.013	0.041	0.026	
Ti	0.476	0.378	0.150	0.382	0.591	0.625	0.400	0.760	0.747	0.737	
Cr	-	-	0.005	0.004	0.000	0.000	0.003	0.008	0.000	0.003	
Σ	5.480	5.455	5.429	5.378	5.249	4.980	5.101	5.260	5.203	5.264	
Ca	0.000	0.000	0.005	0.002	0.003	0.006	0.036	0.005	0.000	0.004	
Na	0.035	0.000	0.184	0.069	0.143	0.184	0.183	0.160	0.126	0.144	
K	1.486	1.544	1.562	1.553	1.602	1.831	1.710	1.574	1.571	1.588	
Σ	1.521	1.544	1.751	1.624	1.748	2.021	1.899	1.742	1.697	1.736	

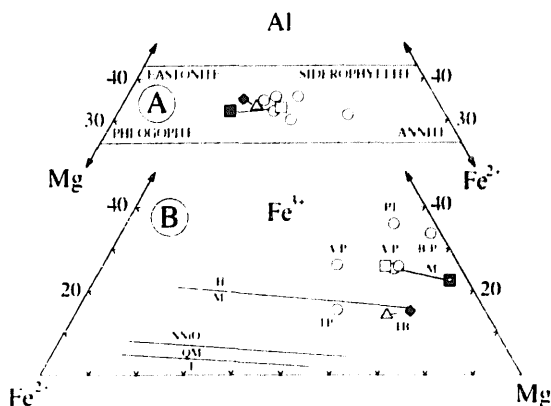


Fig. 5. (A) micas plotted in terms of Al-Mg-Fe²⁺ (22 oxygen basis and assuming total Fe as divalent). (B) micas plotted in the Fe³⁺-Fe²⁺-Mg diagram (Wones and Eugster, 1965; Fe³⁺ from charge balance). Abbreviations and symbols as in Fig. 3.

doleucite pseudomorphs occur in most tephrite-phonotephrite dykes. Pseudoleucite megacrysts are particularly abundant in A-phonolites, while feldspathoids are confined to the groundmass of B-phonolites. Nepheline (Ks=1–20 wt. %) megacrysts, phenocrysts and microlites occur in C- and peralkaline phonolites. Notably, feldspathoids were

not observed in the alkali basalt-trachyphonolite lineage.

Feldspathoid compositions from tephrite-phonotephrite rocks tend to cluster along the Analcime (Anl)-Leucite(Lc) tie line of Petrogeny's Residua System and fall in the primary leucite field, coexisting with Anl-rich compositions in both phonotephrite and phonolite assemblages. Both analcime and pseudoleucite are considered leucite pseudomorphs (cf. Comin-Chiaromonti et al., 1979).

Garnet and sphene. Titanian andradite ($TiO_2 = 3.5\text{--}6.0$ wt. %; andradite = 78–84% mol.) with $Fe^{3+} > Ti$ in the octahedral site and $Al^{IV}/Al^{VI} = 0.5\text{--}0.9$ occurs as microphenocrysts in C- and peralkaline phonolites. A similar garnet composition ($TiO_2 = 2\text{--}6$ wt. %; $Al_2O_3 = 9.8\text{--}7.7$ wt. %; Ferguson, 1978) occurs in a leucite phonolite from the Alban Hills, Roman Region, Ti and Al being negatively correlated from early- to late-crystallized garnet compositions.

While Ti and andradite contents appear to be positively correlated in the garnet from peralkaline phonolites, rims of zoned microphenocryst garnet from C-phonolites tend to be enriched in both Al and Ti, reflecting lower Al and higher Fe^{3+} in the related core compositions. It seems, therefore, pos-

Table 5 - Compositions of amphiboles. Structural formulae on the basis of 23 Oxygens and Fe_2O_3 as from charge balance.

	TEPHRITE		PHONOLITE			TRACHY- PHONOLITE				
	M	GM	C-type		peralkaline			P	GM	
			P	mP	GM	M	P			
SiO ₂	43.28	44.34	38.19	37.67	37.57	36.06	36.59	36.27	38.36	39.11
TiO ₂	4.07	3.79	1.42	2.37	1.98	2.21	2.17	3.20	3.89	4.02
Al ₂ O ₃	9.87	8.78	12.45	12.92	12.81	14.13	13.47	13.82	14.24	13.27
FeO ¹	9.90	9.64	22.90	21.42	23.02	23.8%	23.34	22.35	15.04	13.84
MnO	0.28	0.09	0.70	0.89	0.99	1.04	0.96	0.83	0.36	0.28
MgO	15.38	15.84	6.64	7.28	6.32	5.38	5.77	6.12	10.27	11.38
CaO	12.32	11.46	10.97	11.37	11.13	11.23	10.99	11.38	11.86	11.80
Na ₂ O	2.40	2.48	2.40	2.08	2.10	2.10	2.26	2.16	2.19	2.16
K ₂ O	1.63	1.68	2.49	2.49	2.52	2.60	2.49	2.37	2.10	2.12
Σ	99.13	98.10	98.16	98.49	98.44	98.55	98.04	98.50	98.31	98.18
Fe ₂ O ₃	0.14	0.00	3.12	3.51	3.87	4.31	3.69	2.91	0.67	1.01
Si	6.293	6.479	5.975	5.839	5.866	5.658	5.759	5.667	5.791	5.869
Al IV	1.692	1.513	2.025	2.161	2.134	2.342	2.241	2.333	2.209	2.131
Ti	0.015	0.008	0.000	0.000	0.000	0.000	0.000	0.000	0.000	0.000
Σ	8.000	8.000	8.000	8.000	8.000	8.000	8.000	8.000	8.000	8.000
Al VI	0.000	0.000	0.271	0.200	0.224	0.272	0.258	0.213	0.235	0.216
Fe++	1.188	1.178	2.629	2.367	2.552	2.615	2.636	2.578	1.823	1.623
Fe+++	0.015	0.000	0.368	0.410	0.454	0.508	0.437	0.342	0.076	0.114
Mg	3.333	3.449	1.548	1.602	1.471	1.258	1.353	1.425	2.311	2.590
Mn	0.034	0.011	0.093	0.117	0.131	0.138	0.128	0.110	0.046	0.036
Ti	0.430	0.409	0.167	0.276	0.233	0.261	0.257	0.376	0.442	0.454
Σ	5.000	5.047	5.076	5.052	5.065	5.052	5.069	5.044	5.023	5.033
Ca	1.919	1.794	1.839	1.889	1.862	1.888	1.853	1.905	1.918	1.897
Na	0.676	0.703	0.728	0.625	0.636	0.639	0.690	0.654	0.641	0.629
K	0.302	0.313	0.497	0.492	0.502	0.521	0.500	0.472	0.404	0.406
Σ	2.987	2.810	3.064	3.006	3.000	3.048	3.043	3.031	2.963	2.932

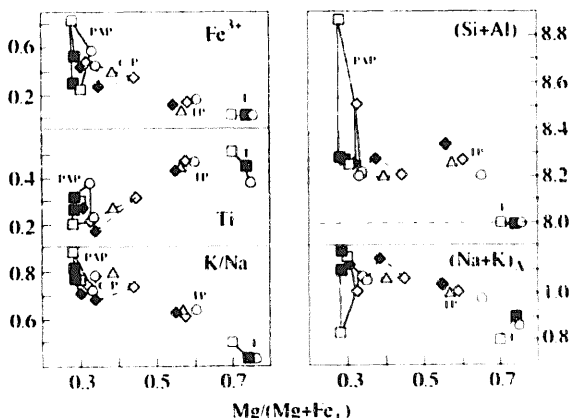


Fig. 6. Amphiboles plotted in terms of atomic Mg/(Mg+Fe_{total}) versus K/Na, Ti, Fe³⁺, (Na+K)/Al and Si+Al. Abbreviations and symbols as in Fig. 3.

sible that the garnet in C-phonolites may be xenocryst.

Microphenocryst sphene is also a ubiquitous accessory of C-type and peralkaline phonolites and in trachyphonolite. Major element contents are relatively constant ($\text{SiO}_2 = 30.0\text{--}30.8$; $\text{TiO}_2 = 38.0\text{--}38.6$; $\text{CaO} 26.4\text{--}27.4$ wt. %); however significant Nb variations were detected ($\text{Nb}_2\text{O}_5 = 0.27\text{--}0.41$ wt. %), which correlate with bulk-rock Nb content.

Significance of the mineralogy

Strong chemical affinities have been documented between major and minor phases in the Sapucai dykes and their analogues from Roman Region. Consistent with the clinopyroxene from Roman Region lavas, the clinopyroxene from the tephrite-phonolite lineage indicates crystallization from metaluminous liquids in its T site configuration and characteristic Al- and Ca-enrichment trend typical of leucitite crystallization residua, i.e. liquids with $(\text{Na}+\text{K})/\text{Al} > 1.0$ and relatively high Ti/Al ratio (Cundari and Ferguson, 1982). The coexisting amphibole reflects these liquids in its T site ($\text{Si}+\text{Al}$) occupancy to 8.00 a.f.u., consistent with increasing $(\text{8-Si})/\text{Al}_{(\text{total})}$ ratio with increasing $(\text{Na}+\text{K})/\text{Al}$ of the bulk rock, documented in leucite-bearing rocks from different tectonic regimes (Ferguson, 1978).

The common occurrence of olivine and its broad equilibrium relationship with the coexisting clinopyroxene in tephrite/phonolite assemblages is con-

sistent with the differentiation controls of the southwestern Uganda (Bufumbira) leucite-tephrite series (Ferguson and Cundari, 1975). This contrasts with the evolution of the Roman Region lavas, where plagioclase+leucite played a dominant role in the differentiation of the tephritic magmas (Cundari and Mattias, 1974; Cundari, 1975, 1979; Holm, 1982). Therefore, the differentiation history of the Sapucai magmas remained largely within the stability fields of the ferromagnesian phases, notably olivine+pyroxene, in the system $\text{Mg}_2\text{SiO}_4\text{--KAlSiO}_4\text{--SiO}_2$ (cf. Edgar, 1980), suggesting that a relatively high-temperature subvolcanic regime prevailed in the Sapucai magmas, compared to that of the Roman Region.

The extreme differentiates from both tephrite-phonolite and alkali basalt-trachyphonolite lineages approach the composition of peralkaline residua, suggesting an extended subvolcanic crystallization history of K-rich, aluminous phases like phlogopite and leucite, at least for the tephrite-phonolite lineage (cf. Cundari and Ferguson, 1982). The phonolitic assemblages may have developed from peralkaline precursor, as documented for the Cordon Complex of the Philippine arc system (Knittel and Cundari, 1990). The widespread occurrence of megacryst/phenocryst, probably xenocrysts phases, points to crystal/liquid mixing from chemically distinct magma batches during their ascent to the surface. Substantial evidence supporting this processes is available from the Roman Region and elsewhere (e.g. Barbieri et al., 1988; Knittel and Cundari, 1990).

Geochemistry

Major and trace elements

Among the wide range of compositions represented in the Sapucai dykes, only representative analyses are given in Table 6 to illustrate the compositional variation of the main rock-types with Mg-values ≥ 0.48 .

In the total alkali-silica and K_2O -silica diagrams (Fig. 7) the shaded fields show the more alkaline character of the tephrite-phonolite lineage in comparison with the alkali basalt-trachyphonolite lineage (cf. also Fig. 2). In the latter, rock-types with $\text{K}_2\text{O}/\text{Na}_2\text{O}$ ratio ≤ 1 are frequent (shoshonitic to

Table 6 - Representative whole-rock compositions, recalculated to 100% on anhydrous basis with total Fe as FeO. Original Fe₂O₃, FeO, L.O.I. and sums are also given.

MINETTE	TEPHRITE				PHONOTEPHRITE				A-PHONO-LILITE				ALKALIBASALT				TRACHY-BASALT			
	1-3088	2-176	3-113	4-3380	5-111	6-3398	7-34	8-50	9-47	10-43	11-28	12-64	13-102	14-248	15-130	16-159	17-129	18-1368		
SiO ₂	48.92	51.16	51.29	50.46	50.23	48.23	46.49	49.43	51.16	49.67	50.11	51.37	48.89	48.21	51.16	49.14	50.75	54.87		
TiO ₂	1.69	1.38	1.37	1.24	1.62	1.78	1.45	1.51	1.59	1.57	1.63	1.84	1.97	1.25	1.04	1.16	1.07	1.07		
Al ₂ O ₃	13.02	14.09	14.17	15.24	13.65	15.11	13.45	15.08	16.41	16.51	18.15	16.56	16.49	15.30	16.68	16.12	16.95	18.25		
FeO [#]	8.30	8.57	8.30	8.81	9.50	9.96	11.91	9.59	8.27	8.37	9.15	8.49	10.77	9.03	10.31	9.68	9.68	6.84		
MnO [#]	0.16	0.14	0.14	0.16	0.14	0.16	0.19	0.16	0.15	0.16	0.16	0.15	0.15	0.18	0.19	0.19	0.14	0.14		
MgO	10.22	8.34	7.78	7.22	7.75	7.32	6.80	5.29	5.68	4.16	4.19	3.88	8.44	5.37	6.43	4.86	3.00			
CaO	9.79	7.64	8.07	9.14	9.04	10.20	10.73	9.06	7.77	8.63	7.54	6.84	6.99	10.34	9.45	6.52				
Na ₂ O	3.20	3.00	3.64	3.84	2.81	2.54	3.48	2.92	3.48	3.41	4.13	3.61	3.80	3.17	3.03	3.43	3.80	4.17		
K ₂ O	4.22	5.55	4.53	3.39	4.86	3.93	4.92	4.92	4.42	5.14	5.89	6.63	2.00	3.18	2.23	2.83	4.59			
P ₂ O ₅	0.54	0.40	0.42	0.50	0.38	0.59	0.36	0.45	0.44	0.61	0.40	0.70	0.34	0.32	0.30	0.34	0.53			
Fe ₂ O ₃	4.48	2.73	4.09	4.47	5.17	3.87	7.05	4.44	3.66	4.17	3.53	6.94	4.15	4.03	3.87	4.66	4.24	1.30		
FeO	3.86	5.58	4.52	4.43	4.48	6.07	4.96	5.18	4.61	5.04	4.61	4.98	2.52	4.43	6.81	5.06	5.62	5.54		
L.O.I.	3.62	2.01	2.95	3.12	1.99	3.08	3.14	2.83	2.42	2.51	1.24	2.84	2.33	1.80	4.30	3.23	3.21	1.02		
Σ	99.79	99.20	99.02	99.52	99.00	99.33	98.84	98.90	99.02	98.92	98.94	99.30	99.06	99.04	99.27	98.81	98.36	99.22		
Cr	395	485	378	275	476	143	190	107	77	95	29	40	53	395	106	160	83	12		
Ni	124	137	96	66	88	67	85	43	27	34	21	24	22	154	37	56	27	7		
Rb	89	129	98	72	108	72	69	107	108	106	105	156	165	109	66	86	88			
Ba	1218	1166	1304	1313	1448	1354	1626	1492	1297	1441	1325	1774	1935	1311	977	1368	1090	1145		
Th	13.2	-	-	-	11.0	28.7	13.8	-	-	10.6	-	12.7	-	-	-	2.8	9.6	31.7		
U	2.6	-	-	-	2.1	6.0	2.7	-	-	2.3	-	3.5	-	-	-	1.4	1.7	9.5		
Ta	3.2	37	31	29	40	30	52	39	43	42	46	41	62	18	20	110	14	37		
Nb	47	37	31	29	22	3.2	3.4	-	-	3.1	-	5.1	-	-	-	1.4	1.2	2.1		
La	88.2	70	66	84	63.3	103.5	77	84	84	94	95	62.2	95	41	23.9	34.4	76			
Ce	165.8	122	128	144	134.6	161.4	133	144	148	163.2	160	185.9	80	87	78.6	87.9	135			
Sr	1216	1249	1452	1375	1816	1200	1913	1856	1933	1903	1429	1626	1288	1409	1336	1456	1412			
Nd	60.6	44	57	53	65	44.1	73.4	58	63	55.2	72	63.2	39	34	73	91	33.4	56		
Eu	22	303	286	212	219	268	251	353	240	360	272	278	365	70	153	-	-	260		
Sm	14.8	-	-	-	12.8	12.4	20.0	-	-	13.3	-	13.9	-	-	-	9.2	9.7	11.2		
Tb	0.8	-	-	-	0.7	1.1	0.7	-	-	0.9	-	0.6	-	-	-	0.6	0.7	0.9		
Y	15.9	16	10	11	9.2	9.6	29.2	16	19	19	19	17.6	23	25	7	17	4.2	20		
Yb	1.7	-	-	-	-	2.0	1.7	-	-	-	-	1.3	-	0.3	-	-	1.5	2.0		
Lu	0.25	-	-	-	-	0.20	0.25	0.29	-	-	-	0.20	-	-	-	0.17	0.21	0.43		
mg#	0.718	0.675	0.652	0.628	0.627	0.612	0.598	0.594	0.569	0.561	0.505	0.486	0.484	0.618	0.551	0.562	0.599	0.475		
K ₂ O/Na ₂ O	1.32	1.85	1.25	0.88	1.73	1.55	0.99	1.68	1.56	1.40	1.25	1.63	1.63	1.05	0.54	0.54	0.75	1.10		

mg# calculated assuming Fe₂O₃/FeO=0.175.

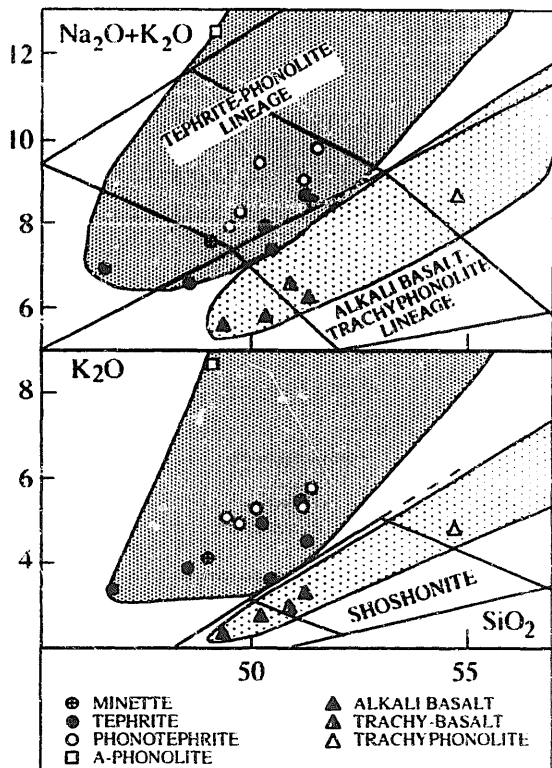


Fig. 7. Sapucai dykes (shaded areas) in the TAS and K_2O - SiO_2 diagrams, as from LeMaitre (1989) and from Beccaluva et al. (1991), respectively. Symbols are for the representative analyses of Table 6 (De La Roche's nomenclature is maintained, minette excepted).

latitic rock-types, according to Le Maitre, 1989).

In general, Mg-values ($Mg\#$), as well as Ni and Cr contents are relatively low and even in those rock-types where $Mg\#$ is in the range of the primitive, mantle-derived magmas ($Mg\#=0.63-0.73$, according to Green, 1971), the Ni ranges between 66 and 154 ppm, 235–400 ppm being the content inferred for primitive magmas (Sato, 1977). Therefore all the magma-types representative of the less evolved dykes in the Sapucai area can be considered to some extent to be derivative (cf. Table 6), similar to the Roman Region rock-types (Civetta et al., 1987: high-K suite, $Mg\#=0.60-0.70$, $Cr+Ni=161-369$ ppm; low-K suite, $Mg\text{-value}=0.51-0.67$, $Cr+Ni=43-319$).

The tephrite-phonolite lineage displays higher TiO_2 , K_2O , Zr, Nb, Y and REE contents than those shown by the alkali basalt-trachyphonolite lineage (Table 6). However, variation diagrams, assuming $Mg\#$ as differentiation index (Fig. 8), show very

scattered values and the observed trends, in particular those relative to the tephrite clan, are not indicative of fractional crystallization processes.

Crystal fractionation

Modeling of crystal fractionation involving ten oxide components was performed using the least-squares program XLFrac (Stormer and Nicholls, 1978). All phases which occur in the assumed parent magmas (i.e. those with the highest $Mg\#$ and $Cr+Ni$ contents) were considered as fractionating phases, including olivine in the minette, because its absence can be the consequence of a reaction relationship with decreasing temperature involving phlogopite and liquid (Luth, 1967; Barton and Hamilton, 1979).

Models with very low sums of the squared residuals ($\sum Sr^2 < 0.5$) relative to alkali basalt-trachyphonolite lineage indicate that the most evolved alkali basalt, trachybasalt and trachyphonolite could be the products of crystal fractionation of olivine+clinopyroxene+plagioclase+magnetite. The trace element modeling (Rayleigh's equation) show that the incompatible elements have calculated/observed ratios generally in the range 0.7–1.30, but Zr and Y display scattered ratios (0.51–1.02 and 0.3–1.85, respectively), probably reflecting different K_D values and the analytical error in low concentrations (Table 6).

The same approach for the *tephrite-phonolite* lineage shows that the dominant fractionating assemblages are olivine+clinopyroxene±phlogopite±leucite±alkali feldspar ($\sum r^2 = 0.10-1.95$) with consequent variable SiO_2 depletions and enrichments in the derivative melts (cf Fig. 8) which evolved in the $Mg_2SiO_4-KAlSiO_4-SiO_2-H_2O$ volume (cf. Hamilton and MacKenzie, 1965; Luth, 1967), as indicated also by the mineralogical features. This is also consistent with different f_{O_2} and a_{H_2O} regimes, expanding the phlogopite volume and suppressing leucite at relatively low pressures (Wallace and Carmichael, 1989; MacDonald et al., 1992).

The scattered calculated/observed ratios relative to the incompatible trace elements are indicative of a more complex typology, i.e. variations of O_2 and H_2O activities, crystal/liquid mixing from distinct magma batches, complex zoning and resorption in mixed potassic magmas, clinopyroxene, foids and/

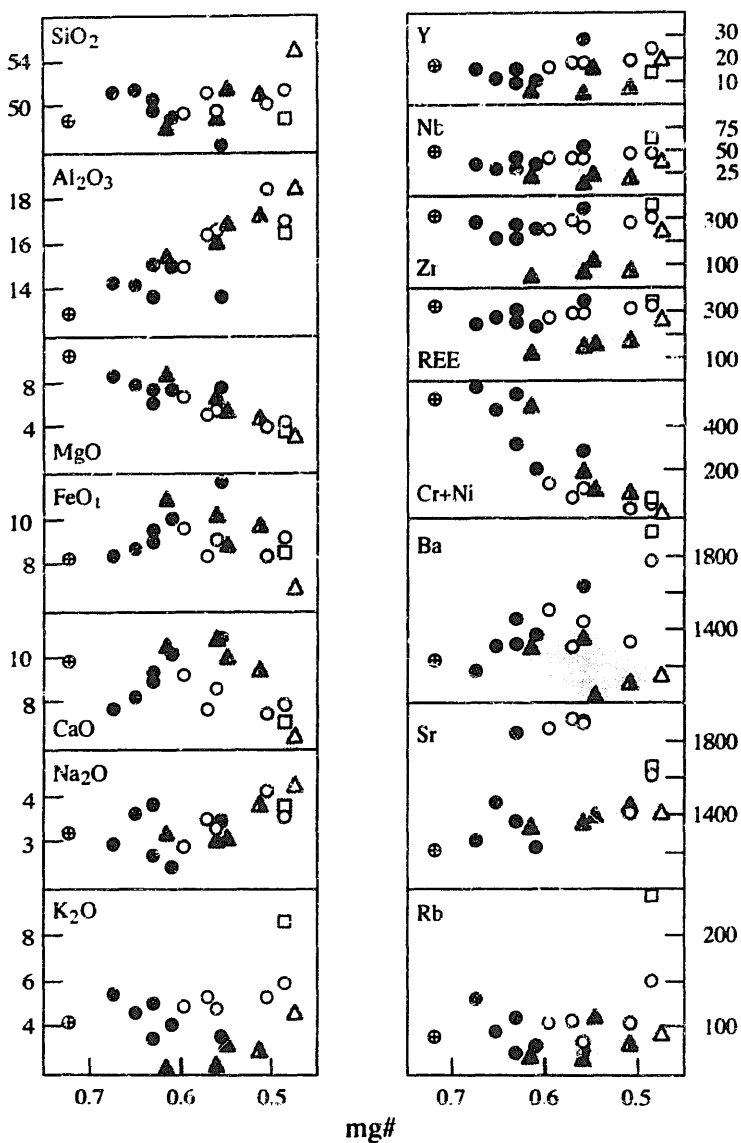


Fig. 8. $Mg/(Mg+Fe^{2+})$, Mg# ($Fe_2O_3/FeO=0.175$) vs. major (wt. %) and trace (ppm) elements variation diagrams for the selected rock-types. Symbols as in Fig. 7. Shaded areas outline the fields from alkali basalt-trachyphonolite lineage.

or phlogopite cumulus, leucite breakdown into pseudoleucite and/or analcimization at low pressure regimes (cf. O'Brien et al., 1988).

Petrogenesis

From the evidence above, the two main lineages of the Sapucai dykes are probably related to distinct parental magmas. Assuming that the least evolved compositions represent derivative liquids, we need to consider compositions with Mg# e.g. between

0.76 and 0.79 (Fo 0.91–0.92 for equilibrium olivine and Ni contents > 240 ppm). Possible compositions are obtained by adding c. 25 wt. % clinopyroxene + olivine (4:1) and 30 wt. % clinopyroxene + olivine (2:1) to minette (Mg# 0.72) and to tephrite (Mg# 0.68) of Table 6, respectively, and 30% clinopyroxene + olivine + plagioclase (6:3:1) to alkali basalt (Mg# 0.62).

Moreover, assuming a garnet peridotite as mantle source (cf Comin-Chiaromonti et al., 1991), for the low Y contents of the observed and calculated

magmas and for strong fractionation between LREE and HREE (and because the spinel peridotite sources indicate melt degree less than 1.5%, up to 0.1%), the melting models (Hanson, 1978) show melt degrees in the ranges 3–7% and 4–7% for the tephrite/minette and alkali basalt clan, respectively, and residual garnet and amphibole in the ranges 2–5% and 0–1%. The model also shows important enrichments and depletions in the mantle source(s) with respect to the primordial mantle of Wood et al. (1979), i.e., (i) *tephrite-phonolite lineage*: Rb, 4–8; Ba, 5–7.5; K, 4–8; Nb, 3.5–6; La, 4–6; Ce, 3.5–5.5; Sr, 2–2.5; P, 1.5–2.5; Zr, 1.5–2.0; Ti, 0.5–1; Y, 0.4–0.7;

(2) *alkali basalt-trachyphonolite lineage*: Rb, 2.5–4; Ba, 5; K, 3.5–4; Nb, 3.5–4; La 3.5–5; Ce, 2.5–3; Sr 2.5–3; P, 1.5; Zr, 1.5–1.7; Ti 0.8; Y, 0.5–0.7.

Notably, garnet peridotite sources are also inferred by melting models for the Mesozoic tholeiitic basalts of Serra Geral Formation (melting degrees: high-Ti basalts, 5–9%; low-Ti basalts, 20%; Piccirillo and Melfi, 1988) and for the Tertiary nephelinites of the Asunción area (melting degrees: 3–6%; Comin-Chiaromonti et al., 1991).

Incompatible element enrichment may be broadly associated with metasomatic processes involving fluids and/or small volume melts (e.g. Menzies et al., 1987; Erlank et al., 1987). Whatever the origin of these fluids, the source was probably in the deeper parts of the lithosphere or upper asthenosphere and such fluids were likely derived from volatile-rich alkaline melts.

Geodynamic significance

The magmatism of the Asunción–Sapucaí graben is an example of potassic volcanism in an intracontinental rifting. In general, Ba and Sr contents of the dykes (Table 6) are relatively high, as might be expected from the potassic character of the dykes. However, not all incompatible elements show enrichments: thus Nb is up to 62 ppm in A-phonolite ($Mg\# = 0.48$). As a result, the ratio of large ion lithophile element/high field strength element (LILE/HFSE) is high: hygromagmatophile element patterns, normalized to primordial mantle (Fig. 9) show strong LILE/HFSE fractionation and negative Ta, Nb, P, Zr, Ti spikes, interpreted by some (e.g. Edgar, 1980; Pearce, 1983; Thompson et al., 1984; Beccaluva et al., 1991) in terms of subduc-

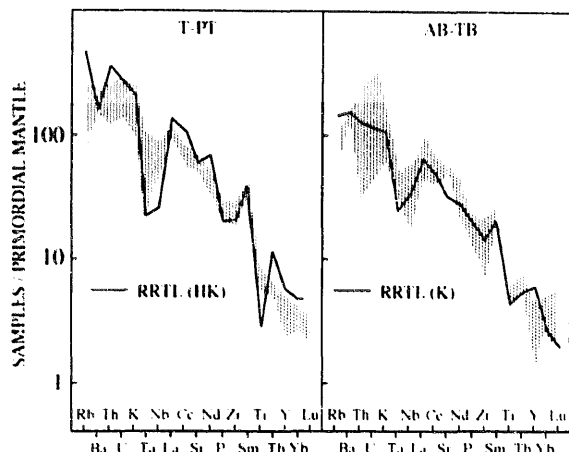


Fig. 9. Primordial mantle-normalized element abundance for the tephrite-phonolite (*T-PT*) and alkali basalt-trachyphonolite (*AB-TB*) lineages, respectively (shaded areas). Normalizing values are from Wood et al., 1979. The averaged compositions of "high potassic", *RRTL(HK)* and "potassic", *RRTL(K)* suites, respectively, from Roman Region lavas are drafted for comparison (source of data: Civetta et al., 1987; Beccaluva et al., 1991).

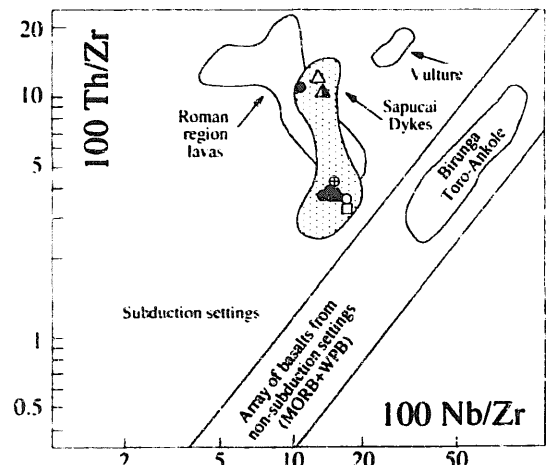


Fig. 10. $100\text{Th}/\text{Zr}$ and $100\text{Nb}/\text{Zr}$ ratios (after Beccaluva et al., 1991; fig. 8, modified) showing the fitting of the selected analyses (Table 6; symbols as in Fig. 7) and the field of the Sapucaí dyke swarm (dashed field: this work and unpublished data).

tion-related processes. The close similarity with generalized patterns for the Roman Region lavas (Barton, 1979; Civetta et al., 1987) is notable.

The Sapucaí compositions are distinct from the field of Ugandan rocks and scatter around the field of Roman Region lavas also in the Th/Zr vs. Nb/Zr diagram (Fig. 10). Also, they fall in a distinct

field, intermediate between the latter and basaltic compositions unrelated to subduction (BCUS), in the Th/Yb vs. Ta/Yb diagram (Fig. 11). Notably, the dykes from Sapucai swarm are on trend with the tholeiitic basalts of the Serra Geral Formation, both groups being distinct from the BCUS. This suggests that the chemical characteristics of the Sapucai dykes may be due to a metasomatized mantle source with Nb-Ta bearing residual phases. This can explain the relatively high and constant $^{87}\text{Sr}/^{86}\text{Sr}$ initial ratios (av. 0.70717 ± 0.00030 at 128 Ma; Velazquez et al., 1992) without intervention of substantial crustal contamination, as also shown by low $\delta^{18}\text{O}\text{\%}(V\text{-SMOW})$ of mica (+4.85 to +5.54), clinopyroxene (+5.09 to +5.20) and whole-rocks (+5.45 to +5.91), according to Marzoli (1991) and by $\delta^{13}\text{C}\text{\%}(PDB-1)$ of the scarce carbonate phases present in the groundmass of the dykes (-5.6 to -6.1; Censi, unpublished data).

Finally, preliminary data relative to the $(^{87}\text{Sr}/^{86}\text{Sr})_0$ (R_0) vs. measured $^{143}\text{Nd}/^{144}\text{Nd}$ variations (Velazquez et al., 1992), show that the lower Cretaceous alkaline magmatism (0.70696 ± 0.00011 vs. 0.51193 ± 0.00003) of the Asunción-Sapucai area is related to mantle sources isotopically distinct from

those of the adjoining tholeiitic flood basalts to the East (Ybyturuzù-Ciudad de Leste area, age 130 Ma; ($R_0 = 0.70587 \pm 0.00009$, $^{143}\text{Nd}/^{144}\text{Nd} = 0.51253 \pm 0.00016$; Marques et al., 1989) and from those of the Tertiary ultrasodic magmatism of the adjoining Asunción area (age 61-39 Ma; $R_0 = 0.70374 \pm 0.00010$, $^{143}\text{Nd}/^{144}\text{Nd} = 0.51274 \pm 0.00006$), the latter also showing pronounced positive Nb spikes (Comin-Chiaromonti et al., 1991a).

The high R_0 values relative to Serra Geral tholeites (i.e. $R_0 \geq 0.706$) were interpreted (Hawkesworth et al., 1986; Macciotta et al., 1990) as the continental extension of the Dupal anomaly, presumably by subduction in a previous orogenic event. Piccirillo et al. (1989, 1990) showed that the tholeiitic basalts, at the Central-Western Paraná Basin, display negligible crustal contamination; moreover, the outpouring of rock-types with low R_0 (≤ 0.704) in the Asunción area would imply the existence of a very thin subduction slab affecting only the potassic magma sources (i.e. $R_0 = 0.707$).

Therefore, the magma production in an area relatively narrow in time and space, reflects more probably lithospheric sources where compositional heterogeneities can be preserved.

Conclusions

The mineral chemistry of the Sapucai dyke assemblages revealed several genetic aspects bearing on the mutual relationships of the corresponding liquids and confirmed established similarities shared by metaluminous potassic lavas from apparently different tectonic regimes, notably the Roman Region. In conclusion, the mineralogy of the Sapucai dykes delineates at least two magma types represented by the *tephrite to phonolite* and *alkali-basalt to trachyphonolite* lineages, or alternatively, to an independent peralkaline forerunner. Transition from peralkaline to metaluminous assemblages may have occurred by interaction of chemically distinct magma batches crystallizing under different f_{O_2} conditions.

The two main lineages are confirmed by the geochemical trends, probably reflecting different metasomatized mantle sources in the lithosphere.

A strong geochemical affinity has emerged between the Sapucai and the leucite-bearing lavas from

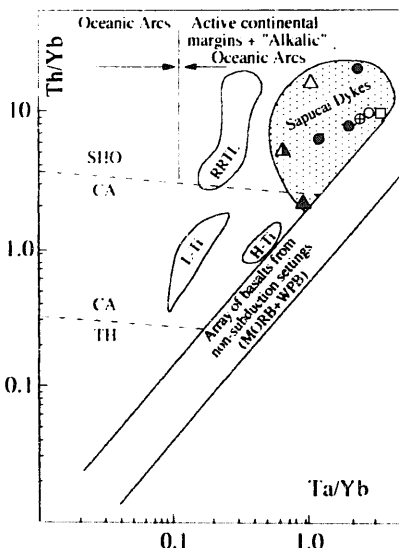


Fig. 11. Th/Yb versus Ta/Yb diagram: *TH*, tholeiitic, *CA*, calc-alkaline, *SHO*, shoshonitic boundaries for arc basalts (Pearce, 1983); *RRTL*, Roman Region type lavas; *L-Ti* and *H-Ti*, low- and high-Ti tholeiites of the Central-Western Paraná basin (source of data: Civetta et al., 1987; Marques et al., 1989; Beccaluva et al., 1991; this work and unpublished data). Symbols as in Fig. 7.

the Roman Region. While the geodynamic significance of this relationships cannot as yet be elucidated in the light of the incomplete petrological and geochemical data on the Sapucaí province, it is clear that Roman Region type magma (Barton, 1979) occurs in a rifted continental setting devoid of orogenic and/or subduction-driven activity. Therefore, a causal relationships of the latter activity with Roman Region type magma is not supported and remains questionable.

Acknowledgements

We thank Dr. B. Upton and Dr. P. Bitschene for the suggestions to improve the paper. Financial support from Brazilian (CNPq, FAPESP and FINAEP) and Italian (CNR and MURST) agencies is gratefully acknowledged. We would like to express our thank to Prof. G. Garbarino for assistance in microprobe analyses and to Prof. R. Alaimo for the facilities in the use of Perkin-Elmer mass spectrometer.

References

- Alaimo, R. and Censi, P., 1992. Quantitative determination of major, minor and trace elements in U.S.G.S. rock standards by inductively coupled plasma mass spectrometry. *Atom. Spectrosc.*, in press.
- Barbieri, M., Peccerillo, A., Poli, G. and Tolomeo, L., 1988. Major, trace elements and Sr isotopic composition of lavas from Vico volcano (Central Italy) and their evolution in an open system. *Contrib. Mineral. Petrol.*, 99: 487-497.
- Barton, M., 1979. A comparative study of some minerals occurring in the K-rich alkaline rocks of the Leucite-hills, Wyoming, the Vico Vulcano, Italy, and the Toro-Ankole Region, Uganda. *Neues Jahrb. Mineral. Abh.*, 137: 113-134.
- Barton, M. and Hamilton, D.L., 1979. The melting relationships of a madupite from the Leucite Hills, Wyoming, to 30 Kb. *Contrib. Mineral. Petrol.*, 69: 133-142.
- Beccaluva, L., Di Girolamo, P. and Serri, G., 1991. Petrogenesis and tectonic setting of the Roman Volcanic Province, Italy. *Lithos*, 26: 191-221.
- Bellieni, G., Brotzu, P., Comin-Chiaromonti, P., Ernesto, M., Melfi, A.J., Pacca, I.G., Piccirillo, E.M. and Stolfa, D., 1983. Petrological and palaeomagnetic data on the Plateau basalt to rhyolite sequences of the Southern Paraná Basin (Brazil). *An. Acad. Brasil. Cienc.*, 55: 355-383.
- Bergman, S.C., 1987. Lamproites and other potassium-rich igneous rocks: a review of their occurrence, mineralogy and geochemistry. In: J.G. Fitton and B.G.J. Upton (Eds.), *Alkaline Igneous Rocks*. Geol. Soc. London, Spec. Publ., 30: 103-190.
- Bitschene, P., 1987. Mesozoischer und Kanozoischer anogenetischer Magmatismus in Ostparaguay: Arbeiten zur geologie und petrologie zweier Alkaliprovinzen. Ph. D. Dissertation, Heidelberg Univ., 317 pp. (unpubl.)
- Civetta, L., Francalanci, L., Manetti, P. and Peccerillo, A., 1987. Petrological and Geochemical variations across the Roman Comagmatic Province: inference on magma genesis and crust-mantle evolution. *Accad. Lincei*, 86: 250-269.
- Comin-Chiaromonti, P., Meriani, S., Mosca, R. and Sinigoi, S., 1979. On the occurrence of analcime in northeastern Azerbaijan volcanics (northwestern Iran). *Lithos*, 12: 187-198.
- Comin-Chiaromonti, P., Gomes, C.B., Piccirillo, E.M., Bellieni, G., Castillo, A.M.C., Demarchi, G., Gallo, P. and Velazquez, Y.C., 1990a. Petrologia do Maciço alcalino de Acahy, Paraguay Oriental. *Rev. Bras. Geocienc.*, 20: 133-152.
- Comin-Chiaromonti, P., Cundari, A., Censi, P., Gomes, C.B., Piccirillo, E.M., Bellieni, G., De Min, A., Orué, D. and Velazquez, V.F., 1990b. Mineral chemistry and its genetic significance of major and accessory minerals from a potassic dyke swarm in the Sapucaí graben, Central-Eastern Paraguay. *Geochim. Brasil.*, 4: 175-206.
- Comin-Chiaromonti, P., Civetta, L., Petrini, R., Piccirillo, E.M., Bellieni, G., Censi, P., Bitschene, P., Demarchi, G., De Min, A., Gomes, C.B., Castillo, A.M.C. and Velazquez, J.C., 1991. Tertiary nephelinitic magmatism in eastern Paraguay: petrology, Sr-Nd isotopes and genetic relationships with associated spinel-peridotite xenoliths. *Eur. J. Mineral.*, 3: 507-525.
- Cundari, A., 1975. Mineral chemistry and petrogenetic aspects of the Vico lavas, Roman Volcanic Region, Italy. *Contrib. Mineral. Petrol.*, 53: 129-144.
- Cundari, A., 1979. Petrogenesis of leucite-bearing lavas in the Roman Volcanic Region, Italy. The Sabatini lavas. *Contrib. Mineral. Petrol.*, 70: 9-21.
- Cundari, A., 1982. Petrology of clinopyroxenite ejecta from Somma-Vesuvius and their genetic implications. *Tschermaks Mineral. Petrogr. Mitt.*, 30: 17-35.
- Cundari, A. and Ferguson, A.K., 1982. Significance of the pyroxene chemistry in leucite-bearing and related assemblages. *Tschermaks Mineral. Petrogr. Mitt.*, 30: 189-204.
- Cundari, A. and Mattias, P.P., 1974. Evolution of the Vico lavas, Roman Volcanic Region, Italy. *Bull. Volcanol.*, 38: 98-114.
- Degriff, J.M., 1985. Late Mesozoic crustal extension and rifting on the Western edge of the Paraná basin, Paraguay. *Geol. Soc. Am. Abstr. Programs*, 17: 560.
- Degriff, J.M., Franco, R. and Orué, D., 1981. Interpretación geofísica y geológica del Valle de Ypacaray (Paraguay) y su formación. *Assoc. Geol. Argent.*, 36: 240-256.
- De La Roche, H., Leterrier, J., Grandclaude, P. and Marchal, M., 1980. A classification of volcanic and plutonic rocks using R1-R2 diagram and major-element analyses. Its relationships with current nomenclature. *Chem. Geol.*, 29: 183-210.
- Druecker, M.D. and Gay, S.P., 1987. Mafic dyke swarms as-

- sociated with Mesozoic rifting in Eastern Paraguay, South America. In: H.C. Halls and W.F. Fahrig (Editors), Mafic Dyke Swarms. Geol. Assoc. Canada, spec. publ., 34: 187–193.
- Edgar, A.D., 1980. Role of subduction on the genesis of leucite-bearing rocks: discussion. *Contrib. Mineral. Petrol.*, 73: 429–431.
- Erlank, A.J., Waters, F.G., Hawkesworth, C.J., Haggerty, S.E., Allsopp, H.L., Rickard, R.S. and Menzies, M.A., 1987. Evidence for mantle metasomatism in peridotite nodules from the Kimberley pipes, South Africa. In: M.A. Menzies and C.J. Hawkesworth (Editors), Mantle Metasomatism. Academic Press, London, pp. 221–329.
- Ferguson, A.K., 1978. Mineral chemistry and petrological aspects of some leucite-bearing lavas from Bufumbira, SW Uganda, and related assemblages. Ph.D. Thesis, Melbourne Univ., 189 pp.
- Ferguson, A.K. and Cundari, A., 1975. Petrological aspects and evolution of the leucite-bearing lavas from Bufumbira, South West Uganda. *Contrib. Mineral. Petrol.*, 50: 25–46.
- Ferguson, A.K. and Cundari, A., 1982. Feldspar crystallization trends in leucite-bearing and related assemblages. *Contrib. Mineral. Petrol.*, 81: 212–218.
- Foley, S.F., Venturelli, G., Green, D.H. and Toscani, L., 1987. The ultrapotassic rocks: Characteristics, classifications and constraints for petrogenetic models. *Earth-Sci. Rev.*, 24: 81–134.
- Gomes, C.B., Comin-Chiaramonti, P., De Min, A., Melfi, A.J., Bellieni, G., Ernesto, M., Castillo, A.M.C., Velazquez, J.C., Velazquez, V.F. and Piccirillo, E.M., 1989. Atividade fisioniana associada ao complexo alcalino de Sapucaí, Paraguai Oriental. *Geochim. Bras.*, 3, 93–114.
- Green, D.H., 1971. Composition of basaltic magma as indicators of conditions of origin: Application to oceanic volcanism. *Philos. Trans. R. Soc. London*, A268: 707–725.
- Hamilton, D.L. and MacKenzie, W.S., 1965. Phase equilibrium studies in the system NaAlSiO₄ (nepheline)–KAlSiO₄ (kalsilite)–SiO₂–H₂O. *Mineral. Mag.*, 34: 214–231.
- Hanson, G.N., 1978. The application of trace elements to the petrogenesis of igneous rocks of granitic compositions. *Earth Planet. Sci. Lett.*, 38: 26–43.
- Hawkesworth, C.J., Mantovani, M.S.M., Taylor, P.N. and Palacz, Z., 1986. Evidence from the Paraná of South Brazil for a continental contribution to Dupal basalts. *Nature*, 322: 356–359.
- Holm, P.M., 1982. Mineral chemistry of perpotassic lavas of the Vulcini district, the Roman Province, Italy. *Mineral. Mag.*, 46: 379–386.
- Knittel, U. and Cundari, A., 1990. Mineralogical evidence for the derivation of metaluminous potassic rocks from peralkaline precursor: the Cordon syenite complex (Philippines). *Mineral. Petrol.*, 41: 163–183.
- Leake, B.E., 1978. Nomenclature of amphiboles. *Am. Mineral.*, 63: 1023–1052.
- LeMaitre, R.W., 1989. A Classification of Igneous Rocks and Glossary of Terms. Blackwell, Oxford, 193 pp.
- Livieres, R.A. and Quade, H., 1987. Distribución regional y asentamiento tectónico de los complejos alcalinos del Paraguay. *Zbl. Geol. Palaontol.*, Teil, I, H7/8: 791–805.
- Luth, W.C., 1967. Studies in the system KAlSiO₄–Mg₂SiO₄–SiO₂–H₂O: Part 1, Inferred phase relations and petrological applications. *J. Petrol.*, 8: 372–416.
- Macciotta, G.P., Almeida, A., Barbieri, M., Beccaluva, L., Brotzu, P., Coltorti, M., Conte, A., Garbarino, C., Gomes, C.B., Morbidelli, L., Ruberti, E., Siena, F. and Traversa, G., 1990. Petrology of the tephrite–phonolite suite and cognate xenoliths of the Fortaleza district (Ceará, Brazil). *Eur. J. Mineral.*, 2: 687–709.
- MacDonald, R., Upton, B.G.J., Collerson, K.D., Hearn, B.C., Jr. and James, D., 1992. Potassic mafic lavas of the Bearpaw Mountains, Montana: Mineralogy, Chemistry and Origin. *J. Petrol.*, 33: 305–346.
- Mariano, A.N. and Dreucker, M.D., 1985. Alkaline igneous rocks and carbonatites of Paraguay. *Geol. Soc. Am. Abstr. Programs*, 17: 166.
- Marques, L.S., Piccirillo, E.M., Melfi, A.J., Comin-Chiaramonti, P. and Bellieni, G., 1989. Distribuição de terras raras e outros elementos traços em basaltos da Bacia do Paraná (Brasil Meridional). *Geochim. Bras.*, 3: 33–50.
- Marzoli, A., 1991. Studio petrologico e geoquímico di complessi alcalini del rift di Sapucaí (Paraguay). Doctoral dissertation, Trieste Univ., 201 pp. (unpubl.)
- Menzies, M.A., Rogers, N.W., Tindle, A. and Hawkesworth, C.J., 1987. Metasomatic and enrichment processes in lithospheric peridotites, an effect of asthenosphere–lithosphere interaction. In: M.A. Menzies and C.J. Hawkesworth (Editors), Mantle Metasomatism. Academic Press, London, pp. 313–359.
- O'Brien, H.E., Irving, A.J. and McCallum, S., 1988. Complex zoning and resorption in mixed potassic magmas of the Highwood Mountains, Montana. *Am. Mineral.*, 73: 1007–1024.
- Palmieri, J.H., 1973. El complejo alcalino de Sapukai (Paraguay Oriental). Ph.D. Diss., Univ. Salamanca, 319 pp. (unpubl.)
- Pearce, J.A., 1983. Role of the sub-continental lithosphere in magma genesis at active continental margins. In: C.J. Hawkesworth and M.J. Norr (Editors), Continental Basalts and Mantle Xenoliths. Shiva, Nantwich, pp. 230–249.
- Piccirillo, E.M. and Melfi, A.J. (Editors), 1988. The Mesozoic Flood Volcanism of the Paraná Basin: Petrogenetic and Geophysical Aspects. IAG-USP, São Paulo, 600 pp.
- Piccirillo, E.M., Civetta, L., Petrini, R., Longineili, A., Bellieni, G., Comin-Chiaramonti, P., Marques, L.S. and Melfi, A.J., 1989. Regional variations within the Paraná flood basalts (southern Brazil): Evidence for subcontinental mantle heterogeneity and crustal contamination. *Chem. Geol.*, 75: 103–122.
- Piccirillo, E.M., Bellieni, G., Cavazzini, G., Comin-Chiaramonti, P., Petrini, R., Melfi, A.J., Pinse, J.J.P., Zantedeschi, P. and DeMin, A., 1990. Lower Cretaceous dyke swarms from the Ponta Grossa Arch (southeast Brazil): Petrology, Sm–Nd isotopes and genetic relationships with the Paraná flood volcanics. *Chem. Geol.*, 89: 19–48.
- Sato, H., 1977. Nickel content of basaltic magmas: Identification of primary magma and a measure of the degree of olivine fractionation. *Lithos*, 10: 113–120.
- Spencer, K.J. and Lindsley, D.H., 1981. A solution model for

- cocexisting iron-titanium oxides. *Am. Mineral.*, 66: 1189–1201.
- Stormer, J.C.Jr. and Nicholls, J., 1978: XLFRAC: A program for interactive testing of magmatic differentiation models. *Comput. Geosci.*, 4: 143–159.
- Thompson, R.N., Morrison, M.A., Hendry, G.L. and Parry, S.J., 1984. An assessment of the relative roles of crust and mantle in magma genesis: an elemental approach. *Phil. Trans. R. Soc. Lond. A* 310: 549–590.
- Wallace, P. and Carmichael, I.S.E., 1989. Minette lavas and associated leucitites from the Western Front of the Mexican Volcanic Belt: petrology, chemistry, and origin. *Contrib. Mineral. Petrol.*, 103: 470–492.
- Velazquez, V.F., Gomes C.B., Comin-Chiaromonti, P., Petrini, R., Kawashita, K. and Piccirillo, E.M., 1992. Magmatismo alcalino mesozoico na porção centro-oriental do Paraguai: aspectos geocronológicos. *Geochim. Brasil.*, in press.
- Wones, D.R. and Eugster, H.P., 1965. Stability of biotite: experiment, theory and application. *Amer. Mineral.*, 50: 1228–1272.
- Wood, D.A., Tarney, J., Vret, J., Saunders, A.D., Bougault, H., Joron, J.L., Treuil, M., Cann, J.R., 1979. Geochemistry of basalts drilled in the North Atlantic by IPOD Leg 49: implications for mantle heterogeneity. *Earth Planet. Sci. Lett.*, 42: 77–97.